The Astrophysical Journal, 794:8 (7pp), 2014 October 10 doi:10.1088/0004-637X/794/1/8

THE MYSTERY OF SPECTRAL BREAKS: LYMAN CONTINUUM ABSORPTION BY PHOTON–PHOTON PAIR PRODUCTION IN THE *FERMI* GeV SPECTRA OF BRIGHT BLAZARS

Boris E. Stern[1,2] and Juri Poutanen[3,4]
[1] Institute for Nuclear Research, Russian Academy of Sciences, Prospekt 60-letiya Oktyabrya 7a, Moscow 117312, Russia; stern.boris@gmail.com
[2] Astro Space Center, Lebedev Physical Institute, Russian Academy of Sciences, Profsoyuznaya 84/32, Moscow 117997, Russia
[3] Tuorla Observatory, University of Turku, Väisäläntie 20, FI-21500 Piikkiö, Finland; juri.poutanen@utu.fi
[4] Astronomy Division, Department of Physics, FI-90014, University of Oulu, Finland
Received 2013 December 19; accepted 2014 August 3; published 2014 September 18

ABSTRACT

We re-analyze *Fermi*/LAT γ-ray spectra of bright blazars using the new Pass 7 version of the detector response files and detect breaks at ∼5 GeV in the rest-frame spectra of 3C 454.3 and possibly also 4C +21.35, associated with the photon–photon pair production absorption by the He II Lyman continuum (LyC). We also detect significant breaks at ∼20 GeV associated with hydrogen LyC in both the individual spectra and the stacked redshift-corrected spectrum of several bright blazars. The detected breaks in the stacked spectra univocally prove that they are associated with atomic ultraviolet emission features of the quasar broad-line region (BLR). The dominance of the absorption by the hydrogen Ly complex over He II, a small detected optical depth, and break energy consistent with head-on collisions with LyC photons imply that the γ-ray emission site is located within the BLR, but most of the BLR emission comes from a flat disk-like structure producing little opacity. Alternatively, the LyC emission region size might be larger than the BLR size measured from reverberation mapping, and/or the γ-ray emitting region is extended. These solutions would resolve the long-standing issue of how the multi-hundred GeV photons can escape from the emission zone without being absorbed by softer photons.

Key words: black hole physics – BL Lacertae objects: general – galaxies: active – galaxies: jets – gamma rays: general – quasars: emission lines

Online-only material: color figures

1. INTRODUCTION

The spectra of bright blazars obtained by the *Fermi Gamma-Ray Space Telescope* (*Fermi*) Large Area Telescope (LAT) showed clear deviations from a power-law shape (Abdo et al. 2009, 2010). These spectra could not be described by smooth functions such as an exponentially cutoff power law or a log-parabola (lognormal distribution), but were found to be better described by a broken power law. The derived break energies lying in the 1–10 GeV energy range (Abdo et al. 2010; Poutanen & Stern 2010; Harris et al. 2012) were rather stable (Ackermann et al. 2010; Abdo et al. 2011; Stern & Poutanen 2011). Those breaks seemed puzzling: the hypothesis that the break is caused by photon–photon annihilation through $e^{\pm}$ pair production was considered and rejected by Abdo et al. (2010, p. 1282), who argued that "to produce a break in the 1–10 GeV, the photon field should have an energy peaking in the 0.05–0.5 keV range, which excludes the broad-line region peaking in the UV." The conclusion that such large energies of target photons are required was based on an erroneous assumption that the break energy corresponded to the maximum cross-section for pair production.

Poutanen & Stern (2010) suggested that the breaks should actually appear at the energies close to the threshold for a corresponding reaction, where the opacity has a sharp rise. The observed breaks at a few GeV then correspond well (correcting for the redshift) to the Lyman recombination continuum (LyC) and Lyα emission of ionized He. They also showed that the inner part of the broad-line region (BLR) can provide sufficient flux of He II Lyman lines and LyC to provide enough opacity for GeV photons and to produce a spectral break. Poutanen & Stern (2010) further demonstrated that the data for a number of bright blazars are well described by a power-law spectrum modified by the absorption within the BLR. The fits with this model were acceptable and the reduction in χ^2 (compared to a simple power-law model) was very significant. Similar χ^2 could also be achieved with the broken power-law model which, however, does not have any physical basis.

A high significance of the spectral breaks partially results from a null hypothesis for the underlying spectrum, which is assumed to be a power law. However, a typical blazar has a curved spectrum extending over many orders in energy and peaking in the MeV–GeV range. This implies that the spectrum in the *Fermi* energy band should be slightly convex and the power-law null hypothesis gives an overestimated significance of the break. As a more realistic null hypothesis one can take a lognormal distribution (log-parabola), which is the simplest way to introduce a curvature in logarithmic coordinates.

Stern & Poutanen (2011) studied in detail the spectrum of the exceptionally bright flat-spectrum radio quasar (FSRQ) 3C 454.3 and indeed found that the spectrum below the absorption break significantly differs from the power law and can be well described by a log-parabola. With this null hypothesis the statistical significance of any break is lower than with a power-law hypothesis. However, the absorption break in the time-integrated spectrum of 3C 454.3 was still highly significant and its energy coincided with the predicted one from He II LyC absorption.

While the most of the focus of the cited papers has been on the GeV breaks, Poutanen & Stern (2010) and Stern & Poutanen (2011) also revealed hydrogen LyC breaks at ∼20 GeV, which were less significant and less impressive because of lower photon statistics in that energy range. Actually, it is obvious that in most cases H Ly radiation should produce a stronger absorption feature than He II Ly emission. That is why it is important to revisit the spectral analysis of bright blazars with

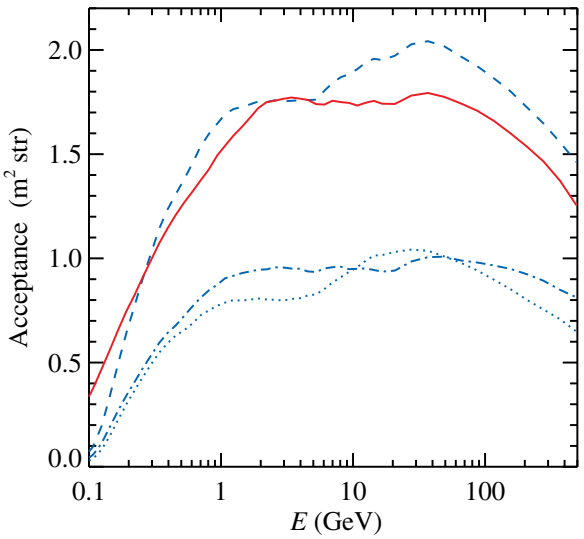

Figure 1. Acceptance (i.e., effective area integrated over the field of view) of *Fermi*/LAT. The solid red curve gives the acceptance for the Pass 7 version `P7_CLEAN_V6`. The blue curves are for the Pass 6 version `P6_V3_DIFFUSE`: the dashed upper curve is the total acceptance for the two detectors—the dotted curve is for the front detector and the dot-dashed curve is for the back detector. The acceptance of the front detector has a hump starting at ~3 GeV and peaking at 30 GeV, which enhances the He II absorption feature or even mimics it.

(A color version of this figure is available in the online journal.)

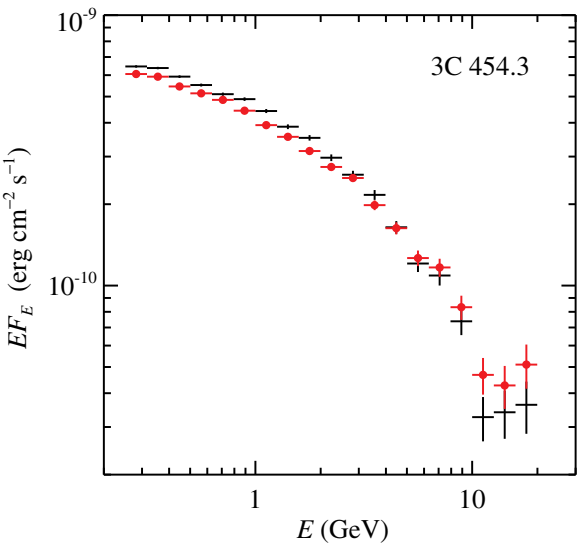

Figure 2. Central part of spectra of 3C 454.3 using response functions for the Pass 6 version `P6_V3_DIFFUSE` (black crosses) and the Pass 7 version `P7_CLEAN_V6` (red circles and crosses).

(A color version of this figure is available in the online journal.)

statistics higher than what was accumulated since previous works. Another, more important reason to revisit previous results is a slight but significant difference in the blazar spectra obtained with the new Pass 7 version of the *Fermi*/LAT data and detector response and those obtained with the older Pass 6 version. The new spectra look smoother, and this is a reason to suspect that the sharp breaks at a few GeV were the artifacts of the Pass 6 response function—partially or completely.

2. DATA AND THEIR ANALYSIS

We use *Fermi*/LAT photon data for 1740 days (from 2008 August 6 until 2013 May 12) using the new Pass 7 event classification, selecting photons of clean class, and imposing the cut on the zenith angle at $\theta < 105^\circ$. We used the `P7_CLEAN_V6` response function. The diffuse background was calculated using the background model elaborated by the *Fermi* team.

It should be noted that the Pass 7 response function significantly differs from the Pass 6 one in at least two aspects.

1. It has a wider point-spread function.
2. It has a different effective area function (see Figure 1).

The second fact is of crucial importance for the analysis of the GeV energy breaks because the Pass 6 response has a hump starting at 4–5 GeV, which introduces a break in the photon spectrum at energies close to the He II LyC absorption (see Figure 2 for comparison of the spectra of 3C 454.3 obtained with Passes 6 and 7). The break is not very strong: it changes the index of the power law by ~0.1. If one then fits the resulting spectrum with a broken power law, one obtains a significant break. We believe that the break in the Pass 6 effective area is not real, because there is no clear reason for existence of such a feature at this energy. Moreover, it looks strange that the hump appears only in the effective area of the front detector. The Pass 7 version of the effective area does not have such a feature and looks more natural.

The energy-dependent exposure function was calculated using the spacecraft pointing history:

$$\mathrm{Exposure}(E, \Delta T) = \int_{\Delta T} S(E, \theta(t))\, dt, \qquad (1)$$

where ΔT is the time interval of interest, θ is the angle between the detector axis and the direction to the object, and $S(E, \theta)$ is the detector effective area at energy E. We accumulated counts in the circle centered at the source location with the energy-dependent radius $r(E) = \min\{r_{90}, 4^\circ\}$, where r_{90} is the radius of 90% event containment, which was calculated with the Monte Carlo integration of the point-spread function assuming isotropic distribution of the exposure angle. Then, the number of counts in each energy bin was corrected to the containment factor for $r(E)$.

In order to reveal the absorption features in the blazar emission, we analyzed the spectra of individual bright FSRQs as well as the stacked spectra of various samples. We selected a sample of the 15 brightest objects from the Second *Fermi* catalog (Nolan et al. 2012) using the following criteria.

1. The total number of counts above 1 GeV after background subtraction is above 1800.
2. The signal/background ratio exceeds 2.
3. Known redshift (according to the Second *Fermi* catalog).
4. Classification as an FSRQ, or as a low-synchrotron peak BL Lac if its redshift exceeds 0.5 (which would mean that the latter is probably a misclassified FSRQ).
5. There is no strong source confusion.

The brightest blazar 3C 454.3 was excluded from the stacking analysis and studied only individually because of its exceptional brightness, which is comparable to the total signal from other selected objects. The remaining 14 FSRQs that are bright above 1 GeV constitute Group 1, where we hoped to reveal the 5 GeV absorption break associated with He II LyC emission (Poutanen & Stern 2010).

Table 1
The Brightest GeV Blazars

Object	Group[a]	Redshift	Dates[b]
3C 454.3		0.859	0–1740
4C +55.17	1, 2	0.896	0–1740
PKS 0537−441	1, 2	0.892	0–1740
PKS 2326−502	1	0.518	600–1740
4C +21.35 (PKS 1222+21)	1, 2	0.433	350–1100
PKS B1424−418	1, 2	1.522	1200–1740
PKS 0426−380	1, 2	1.111	0–1740
PKS 0454−234	1, 2	1.003	0–1740
PKS 0727−11	1	1.591	0–800
PKS 1510−08	1, 2	0.360	0–1740
3C 279	1	0.536	0–1300
PKS 1502+106	1, 2	1.893	0–500
B2 1520+31	1	1.484	0–1400
PKS 0235+164	1	0.940	0–400
4C +38.41	1	1.813	0–1740
BL Lacs			
Mrk 421	3	0.030	0–1740
3C 66A	3	0.444	0–1740
S5 0716+714	3	0.310	0–1740
PKS 2155−304	3	0.117	0–1740

Notes.
[a] Group memberships.
[b] The start and the end of the observation measured from MJD 54684 (2008 August 6).

We also selected eight blazars with the highest number of counts above 5 GeV (more than 200 after background subtraction) to be Group 2. This sample was more promising for studying the H LyC absorption break at ∼20 GeV. All such blazars also belong to Group 1, despite the selection being independent.

To optimize the signal-to-noise ratio, we have selected for each blazar a time interval when its flux substantially exceeded the background. The limits of these time intervals are given in Table 1. In order to prepare the stacked spectra, we first derived individual spectra using the energy bins with the width of 0.1 in decimal logarithm. The bin edges were adjusted in such a way that they are the same in the object rest frame. Each spectrum was blueshifted by a factor $(1+z)$. We summed up the obtained spectra with their absolute normalization, so that the spectra of the brighter objects have a larger contribution. Such approach optimizes relative statistical errors. The blazar spectra were modeled with a lognormal function with the superimposed absorption by the BLR emission (see Section 3). We use the opacity computed for different ionization parameters ξ of the BLR as described in Poutanen & Stern (2010). We also checked a simpler monochromatic absorber model (H and He II LyC), which is less realistic but helps to estimate separate contributions of H and He emission.

We also constructed two comparison spectra, where breaks are not expected, to make sure that the detection of the breaks is not an artifact of the detector response. The first one is the stacked redshift-corrected spectrum of four bright BL Lacs (Group 3 in Table 1). The second one is the "empty" sky spectrum. The sky was sliced into 72,000 bins of equal area (1.74×10^{-4} sr) and the photons were collected from the bins where the number of photons above 100 MeV is less than 300; these bins constitute a fraction of about 0.226 of the sky. The main contribution to this spectrum is from the high-energy protons producing pions and a smaller contribution of unresolved BL Lacs.

Statistical errors were treated as Gaussian, except in a few bins at higher energies. Where the number of photons is low, we use the Poisson likelihood, adding $-2\ln P(n,\mu)$ to χ^2 (here n is the number of counts in the bin and μ is the prediction of the model). The number of such bins is small and the meaning of χ^2 is not significantly affected. For the minimization we use the standard code MINUIT from the CERN library.

3. GAMMA-RAY OPACITY

Gamma-ray photons presumably emitted by the relativistic jet emanating from the black hole are strongly beamed. They propagate through the radiation field made by the accretion disk, the BLR and the dusty torus are potentially can be absorbed by photon–photon pair production. The disk radiation moves nearly parallel to the photon beam and therefore does not interact efficiently. The infrared photons from the dust absorb radiation mostly in the TeV range. Thus, the most important source of opacity is the optical/UV (nearly) isotropic radiation from the BLR.

The opacity depends on the BLR spectrum, which is computed using the spectral synthesis code XSTAR (version 2.2; Kallman & Bautista 2001) as described by Poutanen & Stern (2010). We repeat here the basic assumption for completeness. The ionizing spectrum of a quasar is taken as a sum of the standard multi-color accretion disk plus a power law of total luminosity 10% extending to 100 keV (Laor et al. 1997). The BLR clouds are assumed to be simple slabs of constant gas density and a clear view to the ionizing source. The hydrogen column density was fixed at $N_{\rm H}=10^{23}$ cm^{-2} and the BLR spectra were computed for different ionization parameters $\xi=L/(r^2 n_{\rm H})$ varying from $10^{0.5}$ to $10^{2.5}$. If one assumes a dependence of the cloud density on distance from the black hole $n_{\rm H}=10^{10}r_{18}^{-1}$, then $\xi=10\,L_{47}r_{18}^{-1}$, and our ionization range would correspond to the distance interval between 1 and 0.01 pc to the ionizing source for a quasar luminosity $L=10^{47}$ erg s^{-1}.[5] The scaling and the estimated distances are very approximate and are model-dependent.

If the BLR were to emit only one line at energy E_0, the optical depth for a γ-ray photon of energy E through the region of size R filled with isotropic soft photon field of column density $N_{\rm ph}$ would be $\tau_{\gamma\gamma}(E,E_0)=\sigma_{\gamma\gamma}(s)\,\tau_{\rm T}/\sigma_{\rm T}=N_{\rm ph}\sigma_{\gamma\gamma}(s)$, where

$$\tau_{\rm T}=N_{\rm ph}\sigma_{\rm T}=\frac{L_{\rm line}\sigma_{\rm T}}{4\pi RcE_0}=110\frac{L_{\rm line,45}}{R_{18}}\frac{10\ {\rm eV}}{E_0}, \qquad (2)$$

$\sigma_{\rm T}$ is the Thomson cross-section, $L_{\rm line}$ is the line luminosity, $s=EE_0/(m_ec^2)^2$, and $\sigma_{\gamma\gamma}$ is the angle-averaged cross-section for photon–photon pair production (see, e.g., Gould & Schréder 1967; Zdziarski 1988). Note that $\sigma_{\gamma\gamma}$ has threshold $s=1$ (i.e., at $E_{\rm thr}=19.2\ {\rm GeV}/(E_0/13.6\ {\rm eV})$) and has a peak of about $\sigma_{\rm T}/5$ at $E\approx3.5\,E_{\rm thr}$.

The BLR spectrum, of course, contains many lines and recombination continua. One can introduce the cross-section weighted with the photon distribution:

$$\overline{\sigma}_{\gamma\gamma}(E)=\frac{1}{N_{\rm ph}}\int_{s>1}\sigma_{\gamma\gamma}(s)N_{\rm ph}(E_0)dE_0, \qquad (3)$$

where $N_{\rm ph}=\int N_{\rm ph}(E_0)dE_0$. The spectrum transmitted through the BLR is attenuated as $\propto\exp(-\tau_{\gamma\gamma}(E))$, where $\tau_{\gamma\gamma}(E)=\tau_{\rm T}\overline{\sigma}_{\gamma\gamma}(E)/\sigma_{\rm T}$, and $\tau_{\rm T}$ is computed using Equation (2),

[5] We defined $Q=10^x Q_x$ in cgs units.

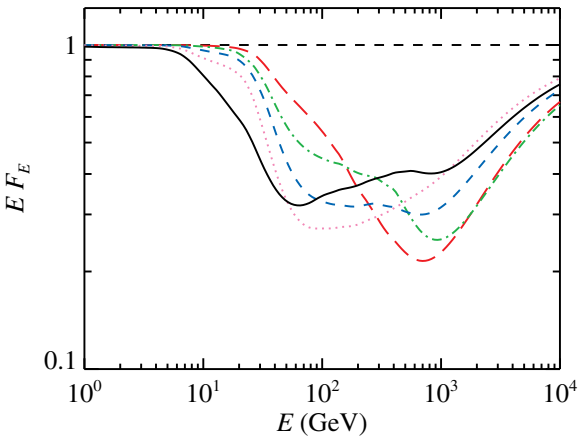

Figure 3. Examples of the photon spectrum transmitted through the BLR of various ionizations and optical depths. The incident spectrum (dashed black line) is taken as a power law of photon index $\Gamma = 2$. The total photon column density corresponds to $\tau_T = 10$ in all cases. Transmission function $\exp(-\tau_{\gamma\gamma}(E))$ for different $\log\xi$ is shown by different lines: 0.5 (red long-dashed), 1.0 (green dot-dashed), 1.5 (blue short-dashed), 2.0 (pink dotted), and 2.5 (black solid).

(A color version of this figure is available in the online journal.)

replacing $L_{\rm line}$ by $L_{\rm BLR}$ and E_0 by the mean photon energy of the BLR:

$$\overline{E} = \frac{1}{N_{\rm ph}} \int E_0 N_{\rm ph}(E_0) dE_0. \quad (4)$$

As an illustration we present the results of absorption of a power-law spectrum by the BLR of different ionizations in Figure 3 fixing the total BLR photon column density at $N_{\rm ph} = 1.5 \times 10^{25}$ cm^{-2}, which corresponds to $\tau_T = 10$. For the considered τ_T, the flux drops at most by a factor of 3–4.5 depending on ξ, corresponding to the maximum optical depth of about 1.1–1.5. Note that the transmitted spectrum in the range from 30 GeV to 1 TeV has nearly the same slope as the intrinsic one at larger ξ, because the opacity is nearly constant in this range. The opacity drops at energies above 1 TeV and the spectrum recovers. We see that the He II LyC breaks at 5 GeV are more pronounced at high ionizations $\log\xi > 1.5$, while the H LyC breaks are seen at any $\log\xi$. This allowed Poutanen & Stern (2010) to introduce a simpler double-absorber model for γ-ray opacity, where the BLR spectrum is replaced by the strongest emission features of H and He II LyC. For low ionization, one can even consider only a single absorber due to the H LyC.

4. RESULTS

4.1. Detection of GeV Breaks

The results of the spectral fits for 3C 454.3, all objects of Group 2, and the stacked spectra are presented in Table 2, and some of them are shown in Figures 4 and 5. The best-fit model for all objects except 3C 454.3 and 4C +21.35 is that of the BLR emission with lower ionization degree $\log\xi = 1.5$. In this ionization state, the contribution by He II absorption is small and one can see from Table 2 that the double-absorber model H+He II LyC does not improve the fits with respect to the single H LyC absorber. This means that in most spectra there is no sign of He II LyC absorption. The exceptions are 3C 454.3 and 4C +21.35 (PKS 1222+21) where the presence of He II absorption is detected at the $\sim 3\sigma$ level. The best-fit model for absorber in these sources is BLR emission with $\log\xi = 2.5$. In the stacked

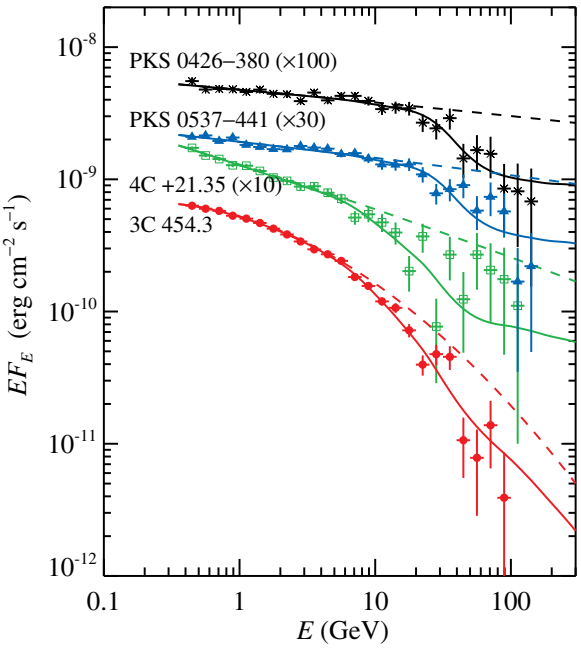

Figure 4. Redshift-corrected *Fermi*/LAT spectra of individual bright blazars and their best-fit model of the lognormal distribution with absorption by the BLR (with $\log\xi = 1.5$). The dashed lines show the same lognormal distributions without absorption.

(A color version of this figure is available in the online journal.)

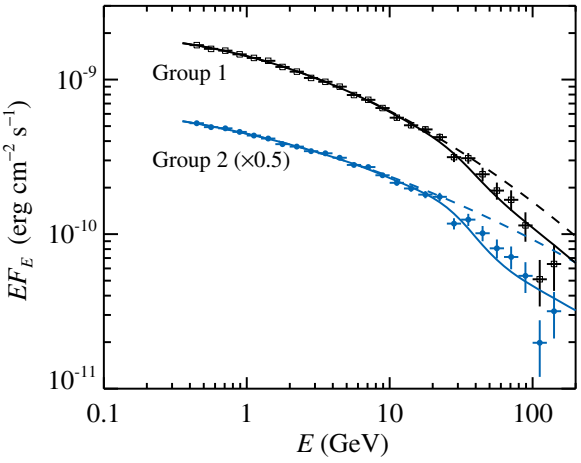

Figure 5. Same as Figure 4, but for the stacked rest-frame spectra for the two samples of blazars from Table 1 for 1740 days of *Fermi* observations.

(A color version of this figure is available in the online journal.)

spectra of both groups, the situation is similar: the addition of He II does not change χ^2 significantly.

The typical optical depth, τ_T, for the best-fit BLR emission model (mostly with $\log\xi = 1.5$) was measured to between 4 and 20. This corresponds to the maximum optical depth of about 0.4–2.2 (see blue dashed line in Figure 3) and the flux reduction at ~100 GeV by a factor of 1.5–9. To estimate the absorption optical depth that is contributed by H and He II emission only, one can consider corresponding optical depths from single- or double-absorber models (see Table 2, Columns 4 and 6).

Spectra of six of the nine brightest (above 5 GeV) blazars demonstrate clear absorption breaks dominated by the H LyC absorption. The significance of these breaks ranges from 2.5σ to 5.5σ. The typical optical depth due to H LyC only is $\tau_H \sim 2$–4, which can be converted directly to the column density of LyC

Table 2
Spectral Properties of Blazars

Object	lognorm	lognorm+H LyC[a]		lognorm+H and He II LyC[b]		lognorm+log $\xi = 1.5$[c]		lognorm+log $\xi = 2.5$[d]		Significance[h]
	χ^2/dof[e]	χ^2/dof[e]	τ_H[f]	χ^2/dof[e]	τ_{HeII}[g]	χ^2/dof[e]	τ_T	χ^2/dof[e]	τ_T	
3C 454.3	55.0/21	38.3/20	4.4 ± 1.0	28.1/19	0.94 ± 0.3	29.6/20	14.0 ± 4.2	25.8/19	8.8 ± 1.7	5.5σ
PKS B1424−418	23.0/23	19.0/22	2.0 ± 1.0	19.0/19	<0.3	18.0/20	6.1 ± 2.9	23.8/20	<4.2	...
PKS 0426−380	42.3/23	27.5/22	3.8 ± 0.7	27.5/21	<0.4	22.9/22	9.6 ± 1.7	36.4/22	6.3 ± 2.6	4.5σ
PKS 1502+106	30.5/21	22.5/20	3.2 ± 1.2	22.5/19	<0.17	21.1/20	9.0 ± 3.3	30.2/20	1.5 ± 1.3	3σ
PKS 0537−441	46.0/23	34.1/22	$3.2^{+1.5}_{-1.0}$	34.1/21	<1.4	29.3/22	9.1 ± 1.5	40.6/22	5.5 ± 2.6	4σ
PKS 0454−234	35.7/23	28.7/22	3.7 ± 1.5	27.5/21	<0.4	28.2/22	10.6 ± 4.5	34.1/22	4.2 ± 3.4	2.5σ
4C +21.35	35.7/22	33.1/21	3.3 ± 2.3	25.5/20	$1.8^{+1.0}_{-0.5}$	33.4/21	25^{+14}_{-21}	23.8/21	11.2 ± 2.5	3.5σ
PKS 1510−08	20.0/21	20.0/20	<0.5	20.0/19	<0.5	20.0/20	<1.4	20.0/20	<0.9	...
4C +55.17	66.0/21	57.9/20	3.1 ± 1.2	57.0/19	<0.8	57.0/20	7.9 ± 2.7	58.0/20	5.6 ± 1.2	...
Group 1	44.0/23	36.8/22	1.0 ± 0.35	36.4/21	<0.05	30.2/22	3.4 ± 1.0	44.0/22	<1.2	3.5σ
Group 2	65.6/23	42.6/22	2.0 ± 0.4	42.6/21	<0.1	31.6/22	6.2 ± 1.1	52.9/22	2.9 ± 1.2	6σ
Group 3 (BL Lacs)	35.4/22	33.7/21	0.37 ± 0.3	33.7/20	<0.1	...	...	...	...	...

Notes.
[a] The lognormal distribution with a single H LyC absorber.
[b] The lognormal distribution with a double absorber, H and He II LyC.
[c] The lognormal distribution with absorption provided by the BLR spectrum with ionization parameter $\log \xi = 1.5$ (see Section 3 and Poutanen & Stern 2010).
[d] Same as case (c), but for $\log \xi = 2.5$.
[e] The number of degrees of freedom (dof) differs because the spectra are cut at the first bin with negative flux.
[f] Optical depth τ_T due to H LyC only.
[g] Optical depth τ_T due to He II LyC only.
[h] The significance of the χ^2 reduction of the best-fit model with respect to the fits with lognormal function.

(plus Lyα) photons on the line of sight to the γ-ray emitting region $N_{\rm ph,H\,LyC} = \tau_H/\sigma_T \approx (3\text{–}6) \times 10^{24}$. The stacked spectrum of Group 2 (which does not include 3C 454.3) has a 6σ significance for the break. This is the most confident and the most conservative demonstration that the H LyC absorption in bright blazars is a very typical phenomenon. Previously, Poutanen & Stern (2010), Stern & Poutanen (2011), and recently Tanaka et al. (2013) revealed this absorption in individual sources. However, in the first and last papers, a less conservative assumption of a power-law null hypothesis was used.

As for the GeV breaks associated with He II absorption (now with a more accurate Pass 7 effective area), they get the status of rare phenomenon. There are indications of such breaks in two objects: 3C 454.3 (3σ) and 4C +21.35 (almost 3σ); see Figure 4.

4.2. Significance of the Breaks

The detection of the breaks due to H LyC absorption has high significance. The amplitude of the spectral deviation from the null hypothesis is factor of two in the case of the stacked spectrum (Group 2) and a factor of three in the case of PKS 0426–380. This is much above the possible systematic errors like uncertainties in the response function.

The breaks due to He II LyC are much weaker than was claimed before (Ackermann et al. 2010; Abdo et al. 2011; Stern & Poutanen 2011), mostly because of the difference between the Pass 6 and Pass 7 detector response functions. A sharp rise in the Pass 6 effective area (see Figure 1) made the spectral break observed at 2–3 GeV sharper and more significant. However, we believe that the breaks observed in two objects, 3C 454.3 and 4C +21.35, are real. First, now there are no features in the LAT response function at the corresponding energy. Second, the deviation of the spectra in the rest-frame range 5–20 GeV from the extrapolation of the lognormal function fitted to the data below 5 GeV reach at least 50% (see Figure 4), much above the uncertainty in the LAT response. It should be noted that the 3σ significance level is quite serious in this case, because detection of the effect does not include "hidden trials" like thresholds

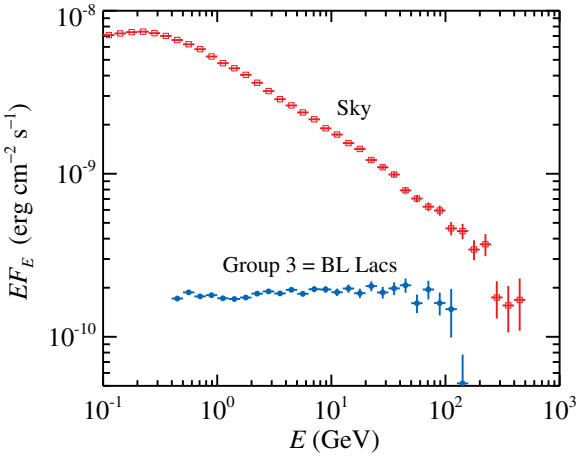

Figure 6. Spectral energy distribution of the "empty" sky is shown by red open squares. The stacked spectrum of the four brightest BL Lacs (Group 3: Mrk 421, 3C 66A, S5 0716+714, and PKS 2155–304) is shown by blue circles. Neither of the spectra shows any signs of absorption by H or He LyC in the range 2–20 GeV.

(A color version of this figure is available in the online journal.)

adjustments and sample manipulation. This significance is also very conservative as it was measured for the lognormal null hypothesis, not a power law. For 3C 454.3, we do not expect systematical errors associated with the background subtraction or source confusion due to exceptionally high γ-ray brightness. 4C +21.35 is weaker and there could be some systematics, e.g., an underestimated soft background: the soft part of the spectrum could be lower and the spectrum could then be fitted with a narrower lognormal distribution without absorption. Therefore, the He II absorption break in 4C +21.35 needs further studies.

In order to prove the presence of the GeV breaks in FSRQ, we checked whether the breaks also appear in the comparison spectra (see Figure 6), where they are not expected. We see that the stacked BL Lac spectrum (Group 3) is well described by

a power law (with some deviations because of the imperfection of the response function) without any breaks (except possibly at 100 GeV). The upper limits on the opacity due to H or He LyC are significantly below the detected opacity in the bright blazars (see Table 2). The "empty" sky spectrum also does not show any signs of the breaks in the 2–20 GeV range. Thus, inaccuracies in the detector response are unlikely to affect our conclusions.

We also made a simple test whether a different null hypothesis for the underlying spectrum would remove the necessity for the breaks. Instead of the lognormal function, we assumed, following the referee's suggestion, a biquadratic function $EF(E) \propto \exp[-A\ln^2(E/E_{\rm peak}) - B\ln^4(E/E_{\rm peak})]$, which has the same number of free parameters as our lognormal distribution with BLR absorption. This ad hoc function gives a slightly better fit with $\chi^2/{\rm dof} = 20/19$ for 3C 454.3, but a much worse fit with $\chi^2/{\rm dof} = 41/22$ for the Group 2 spectrum (see Table 2). Interestingly, a fit for 3C 454.3 gives $A \approx 0$, so that the spectral curvature is fully determined by the quartic term; the physical meaning of such a model is a mystery to us.

5. DISCUSSION AND SUMMARY

Our main results can be formulated as follows.

1. We find that the 20 GeV breaks due to H LyC are ubiquitous. They are statistically significant in the majority of the bright blazars as well as in the stacked redshift-corrected spectra.
2. The 5 GeV breaks due to He II LyC remain significant only in two objects.
3. A more complicated function describing the underlying spectrum can change the significance of the break existence. An ad hoc biquadratic function of $\ln E$ gives a slightly better fit than the physically justified lognormal function with the BLR absorption for 3C 454.3, but a much worse fit for the stacked blazar spectrum. Thus, this model does not eliminate the need for the break.
4. Breaks are not seen in the stacked redshift-corrected BL Lac spectrum or the spectrum of the "empty" sky.
5. The presence of the breaks associated with absorption by UV photons implies that at least some fraction of the γ-rays are produced within the BLR.

The presence of He II LyC absorption in 3C 454.3 is not surprising. This object is exceptional in all its components: the γ-ray emission from the jet reaches luminosities in excess of 2×10^{50} erg s^{-1} (Abdo et al. 2011), the accretion disk emits $L_{\rm d} \sim 10^{47}$ erg s^{-1} (Bonnoli et al. 2011), the BLR 3×10^{45} erg s^{-1} (Pian et al. 2005), and the luminosity in Lyα only is $L_{{\rm Ly}\alpha} \sim 10^{45}$ erg s^{-1} (Wills et al. 1995). Here we can expect that the ionization degree is high and the photon–photon optical depth is substantial.

The second object that shows He II LyC absorption is 4C +21.35. That case is important because this FSRQ has been detected during a flare in the 70–400 GeV range by MAGIC (Aleksić et al. 2011) and the coexistence of the absorption break and very high energy (VHE) emission is difficult to understand in a single emission zone scenario because the multi-hundred GeV photons would have trouble escaping from the BLR. The γ-ray luminosity of 4C +21.35 is smaller than in 3C 454.3, 10^{48} erg s^{-1} during flares (Tanaka et al. 2011), but the accretion disk is almost as luminous with $L_{\rm d} \approx 5\times10^{46}$ erg s^{-1} (Tavecchio et al. 2011). On the other hand, the BLR luminosity is significantly smaller, 5×10^{44} erg s^{-1} (Wang et al. 2004; Fan et al. 2006; Tanaka et al. 2011), with Lyα producing $\sim10^{44}$ erg s^{-1}, i.e., 10 times less than in 3C 454.3. A much lower BLR luminosity implies that the opacity for 100 GeV photons is smaller, because BLR size scales roughly as $R_{\rm BLR} \approx 10^{18} L_{\rm d,47}^{1/2}$ cm (Kaspi et al. 2007; Bentz et al. 2009) and the opacity as $\tau_{\rm T} \propto L_{\rm line}/L_{\rm d}^{1/2}$ (see Equation (2) and Poutanen & Stern 2010). Thus in 4C +21.35, the optical depth through the BLR is expected to be 5–7 times smaller than in 3C 454.3. This might be the reason why VHE emission is detected in 4C +21.35, but not in the much stronger source 3C 454.3.

For a given object having both the measurement of the line luminosity and the estimation of the BLR size, we can obtain an expected value for the opacity $\tau_{\rm T}$ using Equation (2), i.e., assuming that the BLR emission is isotropic and γ-rays have to penetrate through the whole BLR. For 3C 454.3 with $L_{\rm d,47} \sim 1$ and $L_{{\rm Ly}\alpha,45} \sim 1$, we get the opacity from H LyC/Lyα of $\tau_{\rm H} \sim 100$, while for 4C +21.35 we have $\tau_{\rm H} \approx 15$. We see, however, for both objects the observed value is $\tau_{\rm H} \sim 2$–5 (Table 2), much below the expectation. What are the possible solutions for this discrepancy? We can propose at least three solutions.

1. The size of the H LyC/Lyα emission region is larger than that measured from reverberation mapping using C IV (Kaspi et al. 2007) and Hβ lines (Bentz et al. 2009). We note that no Lyα variability was detected in any of the quasars analyzed by Kaspi et al. (2007), supporting this picture. This would immediately reduce the expected γ-ray opacity, which scales inversely proportionally with the size.
2. Alternatively, if the BLR is flat (Shields 1978; Decarli et al. 2011), i.e., elongated along the accretion disk, the γ-ray opacity is much reduced (e.g., Lei & Wang 2014). In this case, the threshold energy, which depends on the maximum interaction angle between the BLR photons and the γ-rays, should be a factor of two larger (i.e., ~40 GeV instead of ~20 GeV), contradicting the data. However, if in addition a few BLR clouds are situated along the jet axis outside the γ-ray emitting region, they would produce enough photons to collide head-on with the γ-rays to create a break at 20 GeV.
3. Finally, the γ-ray emitting region can be extended and its location can change depending on the luminosity, with less GeV absorption during the strong flares (Stern & Poutanen 2011; Pacciani et al. 2014). The VHE emission does not need to be produced in exactly the same place as the GeV emission. This can explain the fact that we see both GeV breaks as well as >100 GeV emission in 4C +21.35 (but not necessarily at the same time).

How then do these models compare with the results on He II absorption? Photoionization models predict that luminosity in He II LyC/Lyα is typically ~10% of the hydrogen one (Tavecchio & Ghisellini 2008; Poutanen & Stern 2010). Thus, taking the same BLR size and geometry and using four times larger photon energy gives $\tau_{\rm He} \sim \tau_{\rm H}/40$. In that case, the He II absorption would be negligible. On the other hand, reverberation mapping shows that He II lines are produced closer to the black hole than, e.g., Hβ (Peterson & Wandel 1999), implying a higher photon density *inside* the zone of complete He ionization and a larger $\tau_{\rm He}$. However, if the γ-ray emitting region is slightly outside of that region the opacity is reduced. Again in this situation the break energy should be higher, but the quality of the data does not allow us to reject a hypothesis that the He II break energy is actually two times larger than the fiducial (rest-frame) 5 GeV value. Thus we do not see an obvious contradiction between the fact that the γ-rays are produced outside (or at the

edge) of the He II LyC emitting region and the presence of the break.

In general, the situation with the H LyC absorption strongly dominating over He II LyC absorption seems more natural than the picture presented by Abdo et al. (2010) and Poutanen & Stern (2010), where the few-GeV breaks look more prominent than those at ∼20 GeV. The statement of Poutanen & Stern (2010) that the jet emission takes place in the inner (higher ionization) regions of BLRs should be modified: the γ-ray emission site lies within the normal H II BLR region. This fact does not change the main astrophysical implications of photon–photon absorption of the jet γ-ray emission; this particularly implies that the jet is already accelerated within a parsec distance from the black hole and therefore the Blandford–Znajek mechanism (Blandford & Znajek 1977; Komissarov et al. 2007) is responsible for the jet launching and the BLR dense photon field can provide conditions for energy dissipation via photon breeding (Stern & Poutanen 2006, 2008).

This research was supported by the Academy of Finland grant 268740 and the Magnus Ehrnrooth foundation. The research made use of public data obtained from the *Fermi* Science Support Center.

REFERENCES

Abdo, A. A., Ackermann, M., Ajello, M., et al. 2009, ApJ, 699, 817
Abdo, A. A., Ackermann, M., Ajello, M., et al. 2010, ApJ, 710, 1271
Abdo, A. A., Ackermann, M., Ajello, M., et al. 2011, ApJL, 733, L26
Ackermann, M., Ajello, M., Baldini, L., et al. 2010, ApJ, 721, 1383
Aleksić, J., Antonelli, L. A., Antoranz, P., et al. 2011, ApJL, 730, L8
Bentz, M. C., Walsh, J. L., Barth, A. J., et al. 2009, ApJ, 705, 199
Blandford, R. D., & Znajek, R. L. 1977, MNRAS, 179, 433
Bonnoli, G., Ghisellini, G., Foschini, L., Tavecchio, F., & Ghirlanda, G. 2011, MNRAS, 410, 368
Decarli, R., Dotti, M., & Treves, A. 2011, MNRAS, 413, 39
Fan, Z., Cao, X., & Gu, M. 2006, ApJ, 646, 8
Gould, R. J., & Schréder, G. P. 1967, PhRv, 155, 1404
Harris, J., Daniel, M. K., & Chadwick, P. M. 2012, ApJ, 761, 2
Kallman, T., & Bautista, M. 2001, ApJS, 133, 221
Kaspi, S., Brandt, W. N., Maoz, D., et al. 2007, ApJ, 659, 997
Komissarov, S. S., Barkov, M. V., Vlahakis, N., & Königl, A. 2007, MNRAS, 380, 51
Laor, A., Fiore, F., Elvis, M., Wilkes, B. J., & McDowell, J. C. 1997, ApJ, 477, 93
Lei, M., & Wang, J. 2014, PASJ, 66, 7
Nolan, P. L., Abdo, A. A., Ackermann, M., et al. 2012, ApJS, 199, 31
Pacciani, L., Tavecchio, F., Donnarumma, I., et al. 2014, ApJ, 790, 45
Peterson, B. M., & Wandel, A. 1999, ApJL, 521, L95
Pian, E., Falomo, R., & Treves, A. 2005, MNRAS, 361, 919
Poutanen, J., & Stern, B. 2010, ApJL, 717, L118
Shields, G. A. 1978, in Proceedings of the Pittsburgh Conference on BL Lac Objects, ed. A. M. Wolfe (Pittsburgh: Univ. Pittsburgh), 257
Stern, B. E., & Poutanen, J. 2006, MNRAS, 372, 1217
Stern, B. E., & Poutanen, J. 2008, MNRAS, 383, 1695
Stern, B. E., & Poutanen, J. 2011, MNRAS, 417, L11
Tanaka, Y. T., Cheung, C. C., Inoue, Y., et al. 2013, ApJL, 777, L18
Tanaka, Y. T., Stawarz, Ł., Thompson, D. J., et al. 2011, ApJ, 733, 19
Tavecchio, F., Becerra-Gonzalez, J., Ghisellini, G., et al. 2011, A&A, 534, A86
Tavecchio, F., & Ghisellini, G. 2008, MNRAS, 386, 945
Wang, J.-M., Luo, B., & Ho, L. C. 2004, ApJL, 615, L9
Wills, B. J., Thompson, K. L., Han, M., et al. 1995, ApJ, 447, 139
Zdziarski, A. A. 1988, ApJ, 335, 786